

Band crossing in Shears band of ^{108}Cd

Santosh Roy*

*S. N. Bose National Centre for Basic Sciences. Block JD,
Sector III, Saltlake City, Kolkata 700098, India*

Pradip Datta†

iThemba Labs, P.O. Box 722 Somerset West 7129, South Africa.

S. Pal,‡ S. Chattopadhyay, S. Bhattacharya, and A. Goswami

Saha Institute of Nuclear Physics, 1/AF Bidhannager Kolkata, 700 064, India

H. C. Jain and P. K. Joshi

*Tata Institute of Fundamental Research,
Homi Bhabha Road, Mumbai 400 005, India*

R. K. Bhowmik, R. Kumar, S. Muralithar, R. P. Singh, N. Madhavan

*Inter University Accelerator Center,
Aruna Asaf Ali Marg, New Delhi 110 067, India*

P. V. Madhusudhana Rao.

Department of Physics, Andra University, Visakhapatnam 530 003, India

(Dated: November 5, 2018)

Abstract

The level lifetimes have been measured for a Shears band of ^{108}Cd which exhibits bandcrossing. The observed level energies and $B(M1)$ rates have been successfully described by a semi-classical geometric model based on shear mechanism. In this geometric model, the bandcrossing in Shears band has been described as the reopening of the angle between the blades of a shear.

PACS numbers: 21.10.Hw, 21.10.Re, 21.10.Tg, 21.60.Ev, 23.20.-g, 25.70.Gh, 27.60.+j

Keywords: Shears band, ^{108}Cd , band crossing, lifetime measurement, semi-classical model

* Also at Saha Institute of Nuclear Physics. 1/AF Bidhannager, Kolkata 700 064, India

† Also at Ananda Mohan College, 102/1 Raja Rammohan Roy Sarani, Kolkata 700 009, India

‡ Presently at IRFU, CEA Saclay, 91191, Gif-sur-Yvette, France

In recent years a large number of Shears band have been identified in mass-100 region [1–6]. The shears structure in these nuclei originate due to proton holes in $g_{9/2}$ orbital and neutron particles in $h_{11/2}/g_{7/2}/d_{5/2}$ orbitals. The bands originating from shears mechanism exhibit sequences of magnetic-dipole (M1) transitions and thus, are often referred to as M1 bands. The observed Routhians and transition rates in these bands have been well described in the framework of Tilted Axis Cranking (TAC) [7, 8] which show that the total angular momentum is almost completely generated by the valance proton and neutron angular momenta. Thus, the different observed features of these Shears bands can also be described successfully by a semi-classical geometric model by Clark and Macchiavelli [3, 9] which involves the coupling of the two angular momentum vectors of protons and neutrons, namely \mathbf{j}_{\perp} and \mathbf{j}_{\parallel} . In this model, the observed band head spin is generated by the perpendicular coupling of \mathbf{j}_{\perp} and \mathbf{j}_{\parallel} . So, at the band head, the angle (θ) between them (called shears angle) is 90° . The higher spin states of the band originate due to gradual closing of these two vectors around their resultant which resembles the closing blades of a pair of shear and the excitation energy along the band increases due to the potential energy associated with reorientation the two vectors. Thus, in this model the highest spin state for a given particle-hole configuration is obtained when the two vectors are fully aligned ($\theta = 0$).

The phenomenon of band crossing in Shears Band is quite similar to that found in the case of collective rotation, i.e at bandcrossing, the observed angular momentum is generated at a lower energy by a new higher quasi-particle configuration [2, 10–12]. However, the two band crossings can be described in two different ways. In case of collective rotation, the bandcrossing is associated to the alignment of a pair of quasi-particles to the rotational axis whose angular momentum adds to the rotational angular momentum. Thus, if the energy needed to break the pair (coupled to zero angular momentum) is lower than that needed to generate the angular momentum through collective rotation, then the bandcrossing is observed. On the other hand, the bandcrossing in Shears band happens due to a new configuration which can reproduce the same angular momentum at a larger shear angle i.e at a lower energy. This happens because the magnitude of the vector(s) or the length(s) of the shear blade(s) increases due to participation of two more particles or holes in forming the new shear structure. The higher angular momentum states after the band crossing are then obtained by re-closing of the newly formed shear blades. Thus, the bandcrossing in Shears band can be related to the reopening of the shear angle.

The validity of this geometric picture can be tested by the measurement of magnetic dipole transition B(M1) rates before and after the band crossing along a Shears band. This rate is proportional to the square of the perpendicular component of the magnetic moment and thus, decrease as the shears close [3]. However, as the shear angle reopens after the band crossing, it is expected that the B(M1) rates will increase immediately after the band crossing followed by the characteristic drop which would indicate the closing of the new shears structure. This feature was observed in ^{196}Pb [10] where the reopening of the shears angle was caused by the alignment of an $i_{13/2}$ neutron pair. Before the band crossing the B(M1) rates were found to drop from 2.4 to $0.7 \mu_N^2$ while after the crossing the values increased to $\sim 9 \mu_N^2$ and drop to $1.8 \mu_N^2$ with increasing spin.

In the mass-100 region, a band crossing in Shears band was first reported in ^{108}Cd by Thorslund *et al.*[13]. This negative parity band (labeled as Band 5 in [13]) comprises of a sequence of ten M1 transitions namely, 121, 316, 522, 677, 466, 362, 482, 590, 706 and 798 keV. Thus, it is apparent that the smooth parabolic behavior of the Shears band is broken after 677 keV transition and a new sequence develops beyond 466 keV transition. The configuration before band crossing was suggested to be $\pi[g_{9/2}^{-2}]_{j=8} \otimes \nu[h_{11/2}^1(g_{7/2}/d_{5/2})^1]$ and the bandcrossing was assigned to $\nu(h_{11/2})^2$ alignment. The lifetimes of the levels in this band were measured by Kelsall *et al.* [2]. In this work, $\pi[g_{9/2}^{-3}g_{7/2}] \otimes \nu[h_{11/2}(g_{7/2}/d_{5/2})]$ configuration was assigned to this band before the neutron alignment based on the observed bandhead energy and B(M1) rates. The measured B(M1) rates showed the characteristic fall as a function of angular momentum after the neutron alignment. However, this fall was not observed before the alignment. Thus, the phenomena of band crossing in Shears band could not be established in ^{108}Cd . In the present work, we have re-measured the level lifetimes of this band by analyzing the observed lineshapes of all the transitions except 121 and 798 keV.

The high spin levels of ^{108}Cd were populated through $^{100}\text{Mo} (^{13}\text{C}, 5n\gamma) ^{108}\text{Cd}$ reaction using 65 MeV ^{13}C beam from 15-UD Pelletron at Inter University Accelerator Centre, New Delhi [14] . The gamma rays were detected by an array of eight compton suppressed Clover detectors. The detectors were mounted on two opposite rings at nominal angles 79° and 139° with respect to the beam direction. The target was made up of 1 mg/cm^2 of enriched (96%) ^{100}Mo backed with a 9 mg/cm^2 natural Pb. The 8×10^8 two-fold coincidence data were sorted in a symmetric and an asymmetric angle dependent matrix using the sorting program

INGASORT [15]. The symmetric matrix was analyzed with RADWARE program ESCL8R [16, 17] to build the level scheme of ^{108}Cd . The present data confirmed the placement of gamma-transitions to the Band 5 of ^{108}Cd as reported in the reference [2].

The asymmetric matrix was analyzed using the program DAMM [18] to extract the lineshapes of the gamma transitions of the Shears Band. The lineshapes were observed above the $I^\pi=13^-$ level and were extracted using the 121 keV gate. The lineshapes of 316 ($I^\pi=14^-$) and 522 ($I^\pi=15^-$) keV transitions were also extracted from 677 ($I^\pi=16^-$) keV gate. The level lifetimes were estimated by using the LINESHAPE analysis code of Wells and Johnson [19]. The analysis procedure has been described in detail in reference [4].

The intensity of the topmost transition namely, 798 keV, was too weak for the lineshape analysis. Thus, the effective lifetime for 21^- was found by fitting the observed lineshape of 704 keV transition by assuming 100% side-fit. The estimated effective lifetime was 0.80(7) ps. For 20^- level, the effective lifetime of 21^- level and side-feeding lifetime were considered as input parameters. The side feeding intensity was fixed to reproduce the observed intensity pattern of the band. In this way, each lower level was added one by one and fitted until all the seven levels were included in a global fit where only the in-band and side feeding lifetimes were allowed to vary. This procedure of global fit was repeated for the forward and backward spectra. The lineshapes of 316 and 522 keV transitions in 677 keV gate were fitted by assuming 100% top-feed with a feeding lifetime equal to the effective lifetime of the 16^- level. The uncertainties in the level lifetimes were derived from the behavior of χ^2 fit in the vicinity of the minimum. Fig. 1 shows the experimental and fitted lineshapes for four gamma transitions in this Band namely 316, 522, 362 and 482 keV. The results of the global fit are summarized in the Table I, where the lifetimes of 14^- and 15^- level were obtained from both 121 and 677 keV gates. It should be noted that the quoted errors do not include systematic error in the stopping power values which may be as large as $\pm 20\%$ [1]. The lifetime of the 14^- level has not been reported by Kelsall *et al.* [2]. In addition, in the present work the lifetime of the 15^- level has been found to be 0.39(4) ps which differs substantially from the previously reported value of 0.69(6) ps [2]. The lifetimes deduced for all other levels are in good agreement with the previously reported values.

The estimated B(M1) transition rates have been deduced from the standard formula [20] and listed in Table I. It is evident from the evaluated B(M1) rates that the values decrease as a function of angular momentum till $I^\pi = 16^-$ and beyond $I^\pi=17^-$ there is a distinct

increase, followed again by a fall. This observation is very similar to that in ^{196}Pb [10] and thus, can be associated with a band crossing in this Shears band.

In order to establish this assumption, the energies and transition rates of the levels of this Shears band have been calculated using the semi-classical model of Shears mechanism [9] and compared with observed values. In this model, the Shears angle (θ) is the important variable which can be derived using the equation

$$\cos\theta = \frac{I_{sh}^2 - j_{\parallel}^2 - j_{\perp}^2}{2 j_{\parallel} j_{\perp}} \quad (1)$$

where, I_{sh} is the shears angular momentum. Thus, the Shears angle associated with a specific level depends on the configuration of the band. Kelsall *et al.*, have established $\pi[g_{9/2}^{-3} g_{7/2}] \otimes \nu[h_{11/2}(g_{7/2}/d_{5/2})]$ as the configuration for this band where two of the proton holes are assumed to be antiparallel and therefore do not contribute to the Shears mechanism [2]. Thus, in the present work, j_{\parallel} has been assumed to be $3.5\hbar$ which corresponds to the $g_{9/2}$ proton hole and $j_{\perp} = 11.5\hbar$ is determined to reproduce the band head spin of $12\hbar$. This contribution comes from $\pi g_{7/2}$ and $\nu[h_{11/2}(g_{7/2}/d_{5/2})]$. After the band crossing, $\pi[g_{9/2}^{-3} g_{7/2}] \otimes \nu[h_{11/2}^3(g_{7/2}/d_{5/2})]$ configuration has been assigned to the new band [2] whose band head spin is $17\hbar$. In order to reproduce this spin, j_{\perp} has been taken to be $16.5\hbar$. It is interesting to note that this assumption is in agreement with the experimental alignment gain of $\sim 5\hbar$ [13].

Under these assumptions, the shears angle has been calculated using Eq. 1 for every angular momentum state of the Shears band and the values are listed in Table II. It is to be noted that the maximum angular momentum for this shears configuration is $20\hbar$ while the band has been observed up to $22\hbar$. This small difference (10%) due to the core rotation is assumed to be a linear function of angular momentum. Thus, $I_{sh} = I - (\Delta R/\Delta I)(I - I_b)$ [1], where I_b is the band head spin ($=12\hbar$) and $(\Delta R/\Delta I)=0.4$ for the present case.

Since the core contribution is small, the energy levels of the band can be calculated following the prescription of Macchiavelli *et al.* [9].

$$E_I - E_b = (3/2)V_2 \cos\theta_I \quad (2)$$

where, E_I is the energy of the level with angular momentum I, and θ_I is the corresponding Shears angle and V_2 is the strength of interaction between the blades of the shear.

Figure 2(a) and (b) show the comparison with the data before and after the band crossing, respectively. The experimental level energies are best reproduced for $V_2 = 1.65$ MeV

before the band crossing and $V_2 = 2.65$ MeV after. It is interesting to note that for the above mentioned configurations, there are three particle-hole combinations before and five combinations after the band crossing. Thus, the interaction strength per pair is ~ 550 keV. This is in good agreement with the observed systematics of ^{110}Cd , where $V_2 = 4$ MeV for eight particle-hole combinations [1]. Thus, the observed systematics of V_2 support the model of re-opening of the shear angle at the band crossing due to participation of two more particles. This picture may be further clarified by calculating the B(M1) rates.

In the Fig. 3, the evaluated B(M1) rates have been plotted as a function of angular momentum. These rates can be calculated in the present framework by [3]

$$B(M1) = \frac{3}{8\pi} j_\pi^2 g_{eff}^2 \sin^2 \theta_\pi \quad (3)$$

where, $g_{eff} = g_\pi - g_\nu$, $j_\pi = 3.5$ and θ_π is related to the shears angle (θ) through

$$\tan \theta_\pi = \frac{j_\nu \sin \theta}{j_\nu \cos \theta + j_\pi} \quad (4)$$

The calculated values of θ_π are tabulated in Table II. The value of g_{eff} before and after the band crossing was found to be 1.13 and 1.22, respectively. In this calculation, the single particle g-factor of $g_{9/2}$ proton, $g_{7/2}$ neutron and $h_{11/2}$ neutron were taken to be 1.27, -0.21 and 0.21 respectively [5] and the normal parity neutron was assumed to have predominantly $g_{7/2}$ character. The calculated values are shown as solid line in Fig. 3. There is a good agreement between the calculated and observed values and the characteristic variation of the B(M1) rate before and after the band crossing has been well reproduced by the semi-classical model. Thus, the observed B(M1) rates are also consistent with the assumption that the band crossing in the Shears band can be described as the reopening of the shears angle.

It is interesting to note that the previously assigned configuration [13] would predict the B(M1) rates to be ~ 4 times higher as for this configuration $j_\pi = 8$ as compared to 3.5 for the present configuration. However, such large B(M1) transition rates have been reported for a Shear band in the immediate even-even neighbor namely, ^{110}Cd [1]. This band was assigned $\pi[g_{9/2}^{-2}] \otimes \nu[h_{11/2}^2(g_{7/2}/d_{5/2})^2]$ configuration by comparing the observed B(M1) rates with TAC calculations. In Fig. 3, the measured values are plotted as open circles. The dotted line represents the calculated values from the present semi-classical model for the above-mentioned configuration and is in good agreement with the observed values. Thus,

the B(M1) rates in the Shears bands in this mass region can be used as a marker for the excitation of protons across the N=50 core as they decrease by a factor of four in case of core excitation.

In summary, the observed band crossing in Shears band of ^{108}Cd can be understood in the following way. The band head spin of $12\hbar$ is formed by two perpendicular vectors of a shear, $\mathbf{j}_{\parallel} = 3.5$ and $\mathbf{j}_{\perp} = 11.5$. The levels up-to $I^{\pi}=16^{-}$, are generated by the closing of the shear angle from 90° to 38° . At $I^{\pi}=17^{-}$, this shear closes and a new shear is formed where two more neutrons join \mathbf{j}_{\perp} . Thus, \mathbf{j}_{\perp} increases to 16.5 and the shear angle reopens to 90° . The higher spin levels up to $22\hbar$ are then generated by gradually closing the blades of this new shear. In this picture, it has been assumed that an angular momentum of $2\hbar$ due to core rotation has been linearly distributed over the levels of this band. Thus, the present work establishes the phenomenon of band crossing in a Shears band in mass-100 region.

The authors would like to thank Professor A. O. Macchiavelli for useful discussion and suggestions. We would also like to thank Professor John Wells for providing the lineshape analysis package and Professor Nimal Singh of Punjab University for providing the target. The authors would also like to acknowledge the efforts of all the technical staffs of the Pelletron facility at IUAC, New Delhi, for smooth operation of the machine.

-
- [1] R.M. Clark *et al.*, Phys. Rev. Lett. **82**, 3220 (1999) .
- [2] N.S. Kelsall *et al.*, Phys. Rev. C **61**, R011301 (1999).
- [3] R.M. Clark and A. O. Macchiavelli, Annu. Rev. Nucl. Part. Sci. **50**, 1 (2000).
- [4] P. Datta *et al.*, Phys. Rev. C **78**, R021306 (2008).
- [5] P. Datta *et al.*, Phys. Rev. C **69**, 044317 (2004).
- [6] P. Datta *et al.*, Phys. Rev. C **67**, 014325 (2003).
- [7] S. Frauendorf, Rev. of Mod. Phys. **73** 463b (2001).
- [8] S. Frauendorf, Nucl. Phys. **A557** 259c (1993).
- [9] A.O. Macchiavelli *et al.*, Phys. Rev. C **57**, R1073 (1998).
- [10] A.K. Singh *et al.*, Phys. Rev. C **66**, 064314 (2002).
- [11] P. Agarwal *et al.*, Phys. Rev. C **76**, 024321 (2007).
- [12] J.R. Cooper *et al.*, Phys. Rev. Lett. **87**, 132503 (2001) .
- [13] I. Thorslund *et al.*, Nucl. Phys. **A564** 285 (1993).
- [14] G.K. Mehta and A. P. Patro, Nucl. Instrum. Methods Phys. Res. A, **268** 334 (1988).
- [15] R.K. Bhowmik *et al.*, 422, DAE Symposium on Nucl. Phys., Vol **44B**, 2001.
- [16] D.C. Radford, Nucl. Instrum. Methods Phys. Res. A **361** 306 (1995).
- [17] D.C. Radford, Nucl. Instrum. Methods Phys. Res. A **361** 297 (1995).
- [18] W.T. Milner Oak Ridge National Laboratory (private communication).
- [19] J.C. Wells and N. R. Johnson, (private communication).
- [20] H. Ejiri and M.J.A. de Voigt, *Gamma Ray and Electron Spectroscopy in Nuclear Physics* (Oxford University Press, Oxford, England, 1987), p. 504.

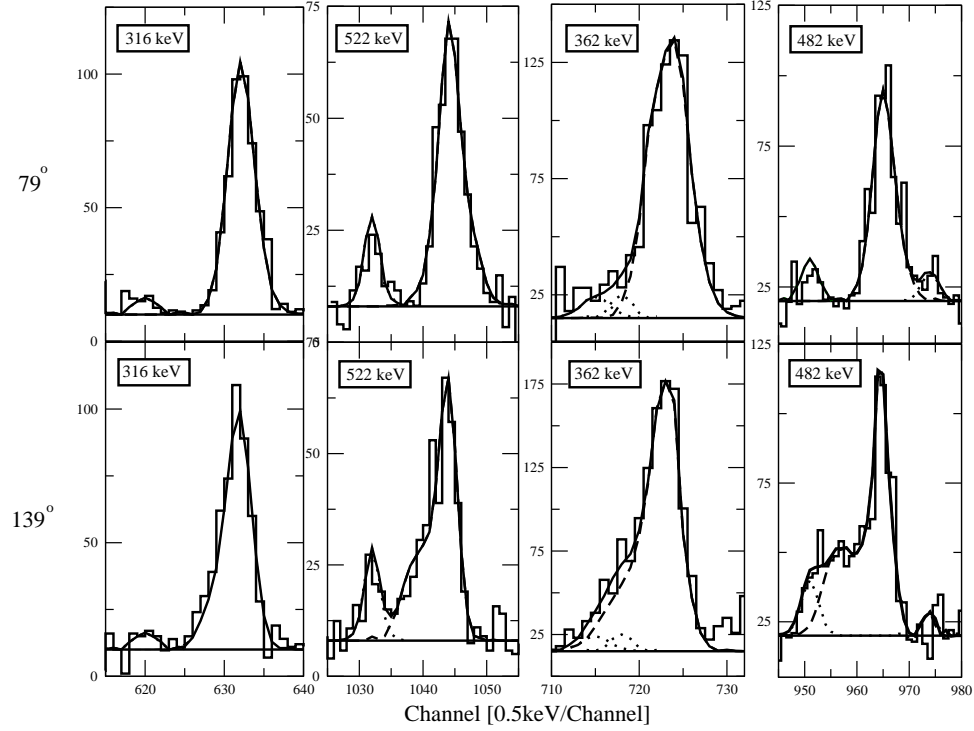


FIG. 1. Experimental and theoretical lineshapes for the 316, 522, 362 and 482 keV γ -rays of ^{108}Cd at 79° and 139° with respect to the beam direction. The contamination peaks are shown by dotted lines and theoretical lineshapes are shown by solid lines.

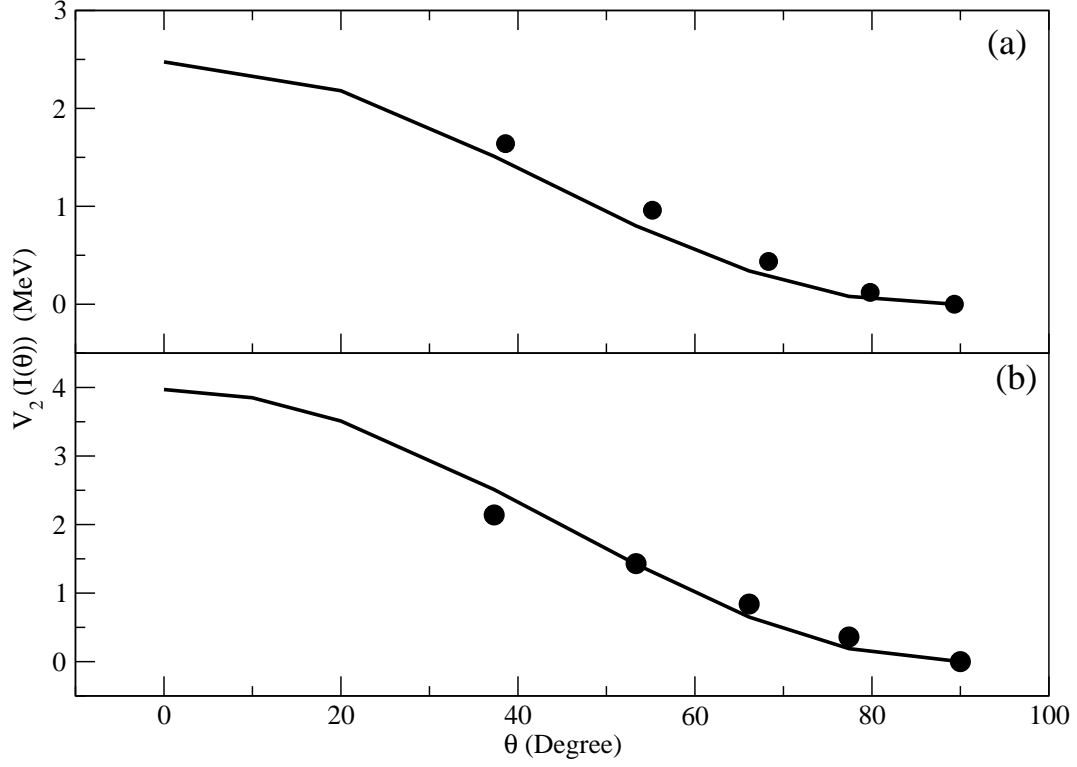


FIG. 2. The effective interaction V_2 between the blades of the shear, \mathbf{j}_{\parallel} and \mathbf{j}_{\perp} , as a function of the shears angle before the band crossing (a) and after (b). The solid line is the fit to the experimental data for (a) $V_2 = 1.65$ MeV and (b) $V_2 = 2.65$ MeV.

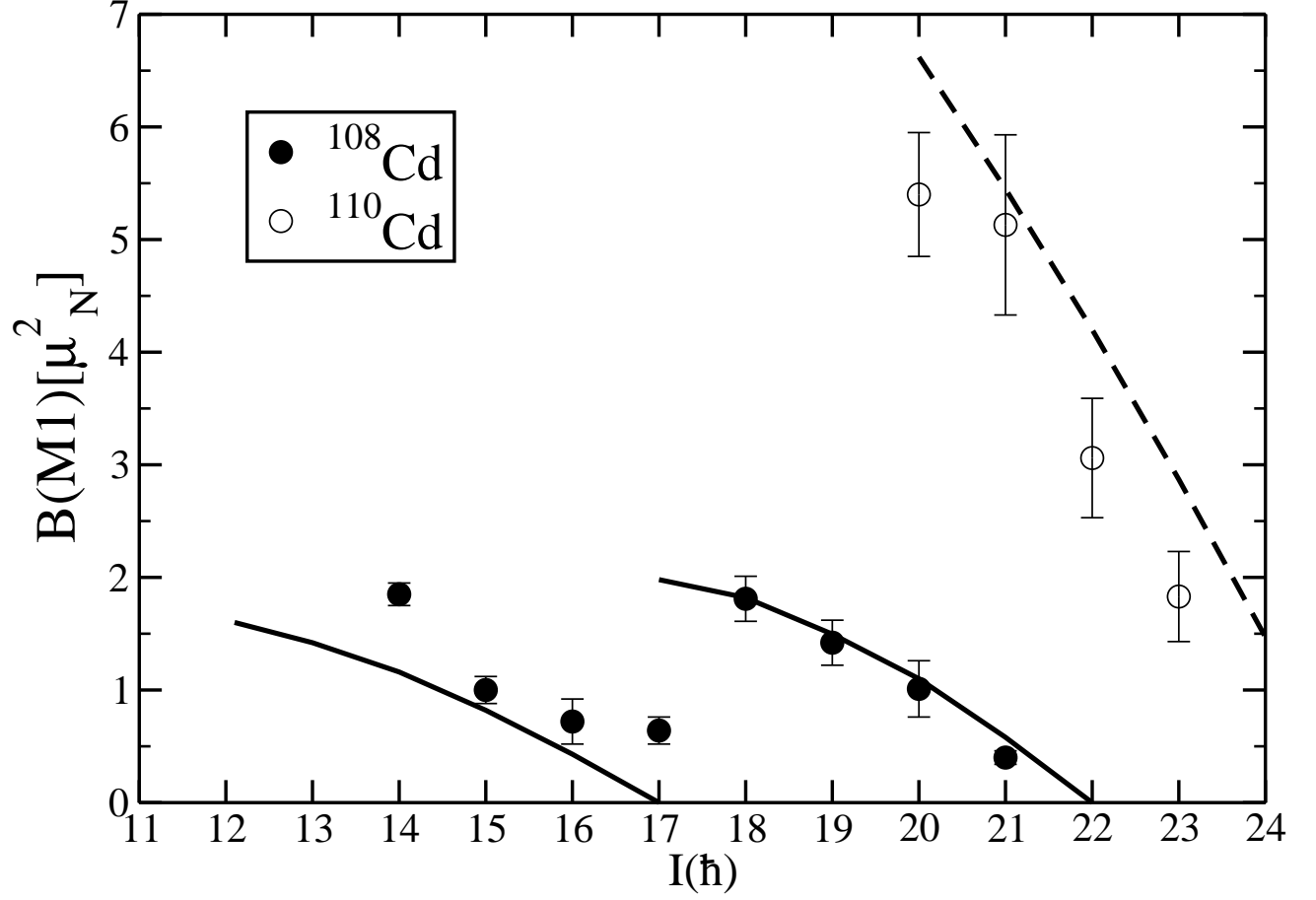


FIG. 3. Experimentally evaluated $B(M1)$ rates as a function of angular momentum in ^{108}Cd and ^{110}Cd [1]. The value for $I^\pi = 22^-$ level in ^{108}Cd has been taken from the reference [2]. The solid and the dashed lines denote the theoretical values from the semiclassical model for ^{108}Cd and ^{110}Cd respectively.

TABLE I. Measured level lifetimes and the corresponding B(M1) transition rates in ^{108}Cd . The error bars on the measured life-times include the fitting errors and errors in side-feeding intensities.

I^π	E_I (keV)	τ (ps)	B(M1) (μ_N^2)
14^-	316	0.95(4)	1.85(10)
15^-	522	0.39(4)	1.0(12)
16^-	677	0.25 (7)	0.72(15)
17^-	466	0.47(6)	0.64(12)
18^-	362	0.65 (6)	1.81(10)
19^-	482	0.30 (6)	1.42(10)
20^-	590	0.23(7)	1.01(15)
21^-	706	0.80(7) ^a	-
22^-	798	-	-

^a Effective level lifetime.

TABLE II. Calculated shears angle (θ) and proton angle (θ_π) for states in Band 5 of ^{108}Cd [13]. $j_\perp=11.5\hbar$ and $j_\parallel=3.5\hbar$ were assumed for $12^- \leq I^\pi \leq 16^-$ and $j_\perp=16.5\hbar$ for higher levels.

I^π	$E_I(\text{keV})$	θ°	θ_π°
12^-	-	89	72
13^-	121	80	64
14^-	316	68	54
15^-	522	55	43
16^-	677	38	30
17^-	466	88	76
18^-	362	77	66
19^-	482	66	56
20^-	590	53	45
21^-	706	37	31
22^-	798	0	0